Preparation of $Y(OH)_3:Eu^{3+}$ and $Y_2O_3:Eu^{3+}$ with Nanotube Morphology by a Facile Hydrothemal Method

BIN DENG[1,a], HAIYING HUANG[1,b], AND RUIJIN YU[2,c]

[1]Department of Chemistry and Life Sciences, Xiangnan University, Chenzhou 423000, P.R. China

[2]College of Science, Northwest A&F University, Yangling 712100, P.R. China

[a]dbhy88@sina.com, [b]xnxyhy@126.com, [c]ddhbyjs@126.com

Keywords: $Y(OH)_3:Eu^{3+}$, $Y_2O_3:Eu^{3+}$, nanotubes, hydrothermal treatment, characterization.

Abstract: In this work, $Y(OH)_3:Eu^{3+}$ nanotubes with 2-3 µm in length and 50-300 nm in diameter have been successfully synthesized on a large scale by hydrothermal treatment of the corresponding oxides in pure water. In addition, $Y_2O_3:Eu^{3+}$ nanotubes could be obtained by calcination of $Y(OH)_3:Eu^{3+}$ nanotubes in air at 450 °C. X-ray powder diffraction(XRD), Field-emission scanning electron microscopic(FE-SEM), transmission electron microscopy(TEM), high-resolution transmission electron microscopy(HRTEM), selected area electron diffraction(SAED), energy-dispersive X-ray spectra(EDS) and the photoluminescence spectra(PL) have been employed to characterize these nanotube materials. The growth mechanism as-prepared nanotubes could be explained well by the highly anisotropic crystal structure of rare earth hydroxides. Advantages of this method were simple, highly reproducible, inexpensive, and widely applicable for the large-scale industrial production.

Introduction

Rare earth compounds have been extensively used in highperformance luminescent devices, magnets, catalysts, and other functional materials because of their optical, electronic, and chemical characteristics, resulting from the 4f shell of their ions[1]. The properties of rare earth compounds depend strongly on their structure, morphology, and composition due to a result of both shape-specific and quantum size effects[2]. Since 1990s, more and more research works are focused on the controllable synthesis of rare earth compounds with low dimension morphology[3], such as nanowire, nanorod or nanotube. The first research on the synthesis of rare earth hydroxide nanotubes was reported by Kijima et al. using polymer-assisted hydrolysis method in solution under hydrothermal condition[4]. Afterward, various rare earth compounds with different morphologies were prepared with different precursors. For example, Qian et al. synthesized yttrium hydroxide nanotubes hydrothermally via a metastable precursor, $PEG-Y(NO_3)_3$[5]. Xu et al. reported a simple route to prepare single-crystal $Dy(OH)_3$ and Dy_2O_3 nanotubes by facile hydrothermal treatment[6]. Li et al. also reported the synthesis of lanthanide hydroxide nanowires through a facile solution-based hydrothermal synthetic pathway based on the preparation of colloidal $Ln(OH)_3$ at room temperature with subsequent hydrothermal treatment at 180°C for about 12 h, including $Dy(OH)_3$, $Sm(OH)_3$, $Tm(OH)_3$, $Nd(OH)_3$, $Pr(OH)_3$, $Gd(OH)_3$, $La(OH)_3$, $Tb(OH)_3$, $Ho(OH)_3$, and $YbO(OH)$ etc.[7,8,9], In the meanwhile, some models or mechanisms have been proposed to explain the crystal growth process. For example, Xu et al. believed that the growth of nanotube was not catalyst-assisted or template-directed, It is likely that the growth is governed by a solution-solid process, in which the oxide molecules were dissolved and hydroxylated from the starting oxide under hydrothermal treatment, subsequently re-crystallized, grew into tubular nanostructures through a dissolution-recrystallization process[1,6]. Li et al. proposed an opinion dealing with the complex interaction and balance between the chemical potential and the rate of ionic motion to explain the optimal pH value for the growth of nanowires[9]. Qian et al. considered that under the hydrothermal condition, the nucleation of $Y(OH)_3$ occurs and there is an intrinsic tendency to grow into rod-like nanoparticles due to its anisotropic hexagonal structure. Subsequently, these nanorods, as the seeds, induce the formation of $Y(OH)_3$ nanotubes[5]. Both the intrinsic structure and favorable kinetic

condition give rise to formation of naotube. However, some of these results are inconsistent. Even now, the exact mechanism for the formation of particles with special morphology is still unclear.

Y_2O_3:Eu^{3+} is a useful red phosphor for lighting and displaying applications[10]. In general, this phosphor is prepared by precipitating yttrium and europium ions with oxalate acid, and then calcining the oxalate at high temperature. The common morphologies are cubic or sheet grains or irregular particles[11]. Here, we reported the preparations of $Y(OH)_3$: Eu^{3+} nanotubes by facile hydrothermal treatment of bulk Y_2O_3:Eu^{3+} powder. Meanwhile Y_2O_3:Eu^{3+} nanotubes were obtained through dehydration of $Y(OH)_3$:Eu^{3+} nanotubes and their photoluminescence properties were also characterized.

Experimental Section

Synthesis. The method for preparation of $Y(OH)_3$:Eu^{3+} nanotubes was as follows: 500 mg of bulk Y_2O_3:Eu^{3+}(3.8%) powder[12] as precursor and 40 ml of distilled water were put into a 50 ml of stainless steel Teflonlined autoclave. The autoclave was sealed and placed in an oven maintained at 170 °C for 30 h. After the reaction was completed, the resulting solid product was filtered and dried at 80 °C in air. Then, $Y(OH)_3$:Eu^{3+} products was obtained. By calcination of $Y(OH)_3$:Eu^{3+} products in air at 450 °C for 6 h, the final products - Y_2O_3:Eu nanotubes were prepared.

Characterization. The phase purity of the products was examined by XRD using a Rigaku/Max-3A X-ray diffractometer with CuKα radiation (λ = 1.5418 Å), the operation voltage and current maintained at 40 kV and 40 mA, respectively. FE-SEM images were obtained with a JEOL JSM-6700F. TEM images, HRTEM images, and SAED patterns were obtained on a JEOL-2010F microscope with an accelerating voltage of 200 kV. EDS was attached to the JEOL 2010F. Sample grids were prepared by sonicating powdered samples in ethanol for 20 min and evaporating one drop of the suspension onto a carbon-coated, holey film supported on a copper grid for TEM measurements. The emission spectra were recorded with an F-4500 spectrophotometer equipped with a 150 W xenon lamp as the excitation source. All the measurements were performed at room temperature.

Results and discussion

The structure and component of the obtained samples have been identified by XRD analyses. Figure 1A and B show the XRD patterns of as-prepared $Y(OH)_3$:Eu^{3+} nanotubes, and Y_2O_3:Eu^{3+} nanotubes, respectively. all the peaks of the XRD patterns in Figure 1A can be readily indexed to hexagonal phase(space group:$P6_3/m$ (176)) of $Y(OH)_3$ with calculated lattice constants a = 6.261 Å and c = 3.544 Å(JCPDS 83-2042), No other impurity phases were detected from XRD analysis, therefore, as-prepared $Y(OH)_3$:Eu^{3+} nanotubes might be free of impurities. In addition, all the peaks of the XRD patterns in Figure 1B could be indexed to a pure cubic phase [space group: Ia $\bar{3}$(206)] of transformed Y_2O_3 with calculated lattice constant of a = 10.602 Å (JCPDS 88-1040). These results clearly showed that the as-prepared $Y(OH)_3$:Eu^{3+} nanotubes were completely converted into Y_2O_3:Eu^{3+} at 450 °C.
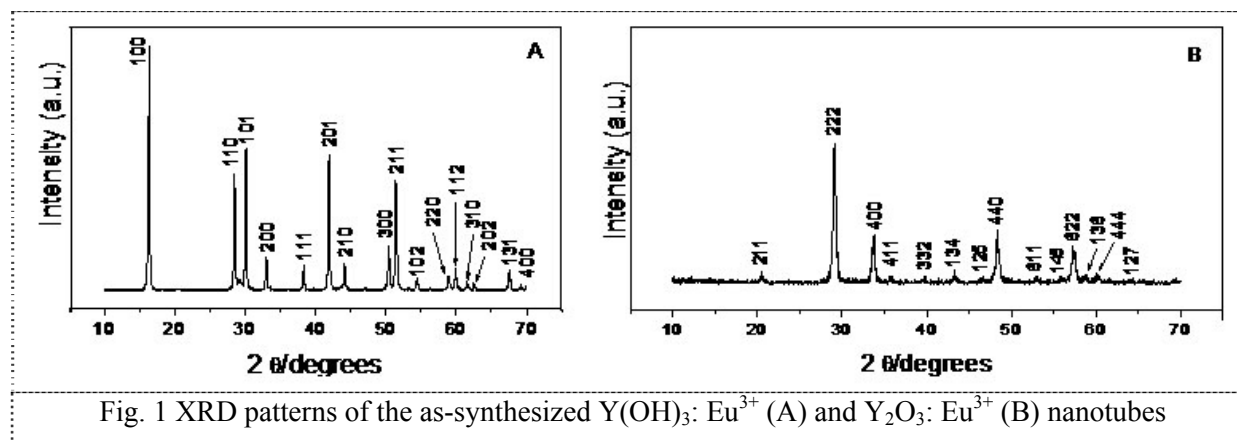

Fig. 1 XRD patterns of the as-synthesized $Y(OH)_3$: Eu^{3+} (A) and Y_2O_3: Eu^{3+} (B) nanotubes

The morphology of the obtained $Y(OH)_3$:Eu^{3+} and Y_2O_3:Eu^{3+} products were characterized by FE-SEM, which could provide information about the quantity and quality of rare earth compound nanotubes. Figure 2 A showed the typical FE-SEM image of the $Y(OH)_3$: Eu^{3+} nanotubes. More than 80 percent of the sample shows nanotube morphology with diameter 50-300 nm and length ranging between 2 and 3 μm. Y_2O_3: Eu^{3+} nanotubes were obtained from the $Y(OH)_3$: Eu^{3+} nanotubes by calcinations at 450°C in air, which was clearly shown some distorted nanotube morphologies in Figure 2B. It could be seen that the tips of these tubes were open ends and had hexagonal prism morphology from Figure 2A and B. We also found that Y_2O_3: Eu^{3+} tubes were smaller than $Y(OH)_3$: Eu^{3+} tubes in that the density of the former was higher than that of the latter. The results demonstrated that $Y(OH)_3$: Eu^{3+} and Y_2O_3: Eu^{3+} nanotubes could be obtained by this simple method.
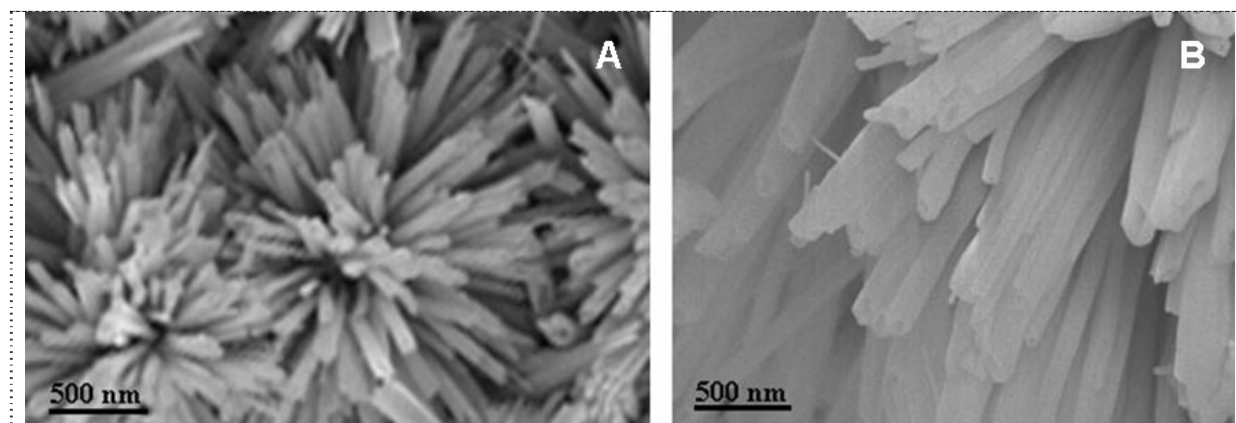
Fig. 2 SEM images of the as-synthesized products: A)$Y(OH)_3$: Eu^{3+} nanotubes and B)Y_2O_3: Eu^{3+} nanotubes.

The morphology, structure and composition of the samples were further examined with TEM, SAED, HRTEM. and EDS. The morphologies of single $Y(OH)_3$: Eu^{3+} and Y_2O_3:Eu^{3+} nanotube were shown in Figure 3 A, and B, respectively. The insets were their corresponding SAED patterns. It could be seen that the $Y(OH)_3$:Eu^{3+} nanotubes were better crystalline than the Y_2O_3: Eu^{3+} nanotubes. Figure 3 C showed the HRTEM patterns of $Y(OH)_3$:Eu^{3+} nanotubes with the clearly resolved interplanar distance $d_{100} = 0.542$ nm, the nanotubes grow along the [001] direction (c axis). HRTEM observations showed that each $Y(OH)_3$:Eu^{3+} nanotube was a single crystal. The Energy dispersive X-ray spectroscopy (EDS) of Y_2O_3: Eu^{3+} nanotubes (see Figure 3D) showed that the nanotube contained Y, Eu, and O elements. The Y_2O_3: Eu^{3+} nanotubes as extracted from the EDS analysis gived a Y/Eu atomic ratio of about 96.31:3.69. It suggested that we have successfully doped Y_2O_3 nanotubes with Eu.

Although the exact mechanism for the formation of $Y(OH)_3$ nanotubes is still unclear, $Y(OH)_3$ nanotubes that were fabricated have a hexagonal crystal structure, similar to that of ZnO, which are well-known to exhibit anisotropic growth. In these solution phase process, the morphology of the product was largely determined by the anisotropic nature. In addition, the physical and chemical ambience of the solution could influence the morphology of the final product. In the growth processes of the $Y(OH)_3$:Eu^{3+} nanotubes, Eu doped $Y(OH)_3$ growed in nanotube the same as $Y(OH)_3$, as the similarity of their crystal structures and lattice constants.

Room-temperature photoluminescence emission spectra were recorded with an F-4500 fluorescence spectrometer using a Xe lamp as the excitation source. Figure 4 presented PL spectra of Y_2O_3:Eu^{3+} nanotubes under 467 nm excitation. The strongest peak at 610 nm was due to the forced electric dipole transition ($^5D_0 \rightarrow {}^7F_2$), which was allowed on condition that the europium ion occupies a site without an inverse center. Its intensity was hypersensitive to crystal environments. The peaks near 590 nm derived from the allowed magnetic dipole transition ($^5D_0 \rightarrow {}^7F_1$)[13], indicating that obtained Y_2O_3:Eu^{3+} nanotubes had a high optical property.
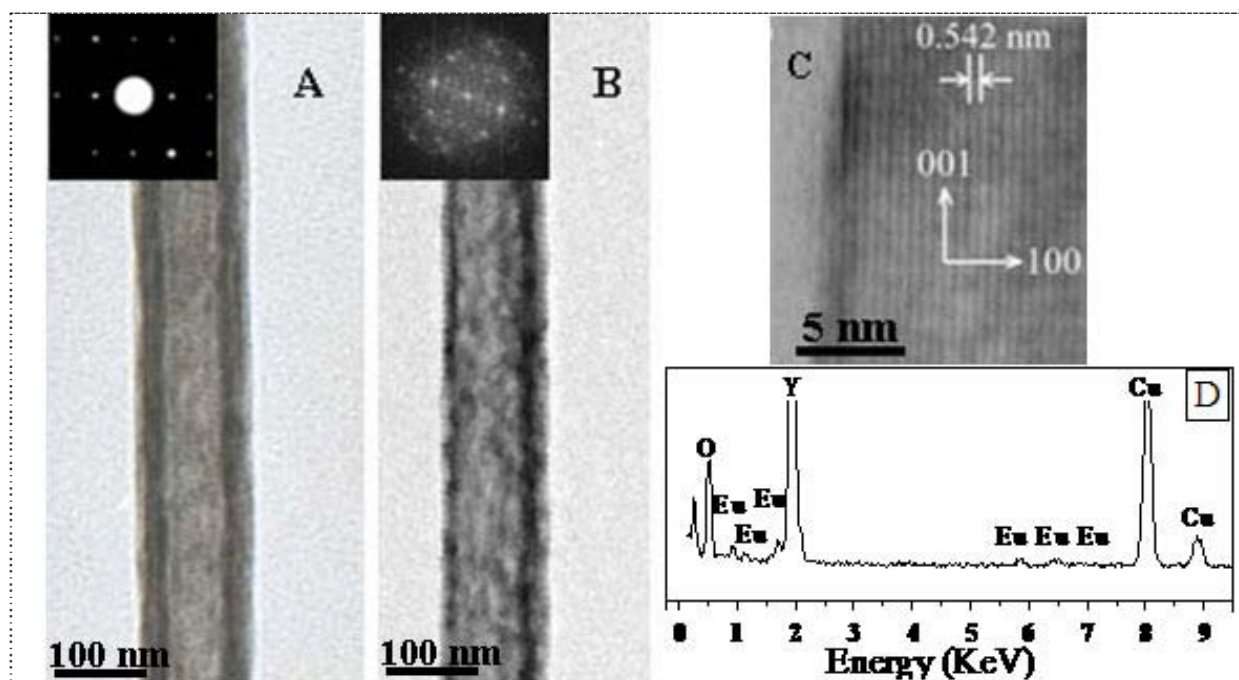
Fig. 3 A) TEM image of a single $Y(OH)_3$:Eu^{3+} nanotube, insets is the SAED pattern; B) TEM image of a single Y_2O_3:Eu^{3+} nanotube, insets is the SAED pattern; C) HRTEM image of $Y(OH)_3$:Eu^{3+} nanotube; D) EDS results of Y_2O_3: Eu^{3+} nanotubes.
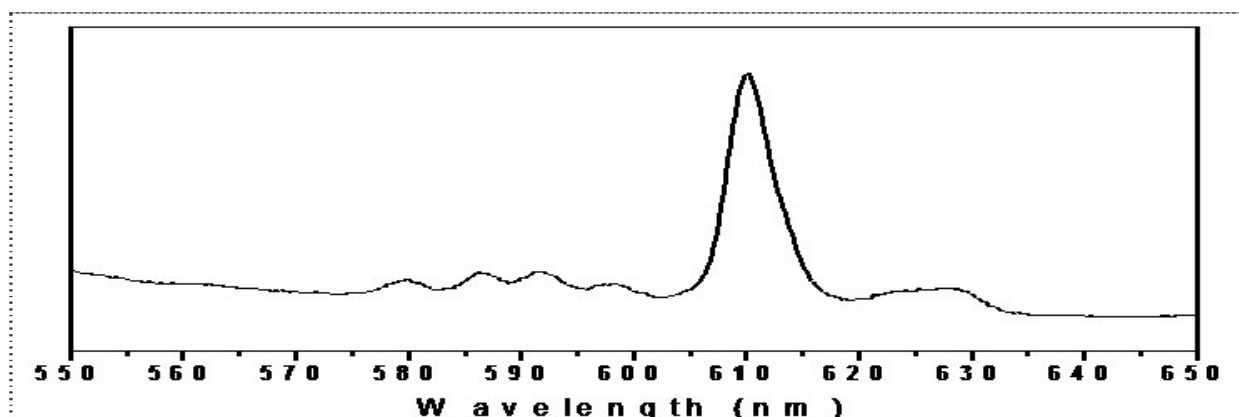

Fig. 4 PL spectra of the as-synthesized Y_2O_3: Eu^{3+} nanotubes

Conclusions

We have successfully synthesized the $Y(OH)_3$: Eu^{3+} nanotubes by facile hydrothermal treatment of bulk Y_2O_3 : Eu^{3+} powder. The as-prepared $Y(OH)_3$: Eu^{3+} nanotube were about 2-3 μm in length and 50 to 300 nm in diameter. Y_2O_3: Eu^{3+} nanotubes could be obtained through dehydration of $Y(OH)_3$: Eu^{3+} nanotubes. Their photoluminescence properties revealed that we had successfully synthesized Y_2O_3:Eu^{3+} nanotubes. It is foreseeable that these novel 1D functional nanostructures with different shapes and sizes will provide further research opportunities in chemistry, physics, and other interdisciplinary fields of science and technology.

Acknowledgements

References

[1] Y. P. Fang, A. W. Xu, L. P. You, R. Q. Song, J. C. Yu, H. X. Zhang, Q. Li, and H .Q. Liu. Adv. Funct. Mater. Vol.13(2003),p.955.

[2] Y. N. Xia, P. D. Yang, Y. G. Sun, Y. Y. Wu, B. Mayers, B. Gates, Y. D. Yin, F. Kim, Y. Q. Yan. Adv. Mater.,Vol. 15(2003).p.353.

[3] R. X. Yan, X. M. Sun, X. Wang, Q. Peng, Y. D. Li. . Chem. Eur. J.Vol. 11(2005),p.2183.

[4] M. Yada, M. Mihara, S. Mouri, M. Kuroki, T. Kijima. Adv. Mater.Vol. 14(2002), p.309.

[5] Q. Tang, Z. P. Liu, S. Liu, S. Y. Zhang, X. M. Liu, Y. T. Qian. J. Cryst. Growth.,Vol. 259(2003), p.208.

[6] A.W. Xu, Y. P. Fang, L. P. You, H. Q. Liu. J. Am. Chem. Soc.Vol. 125(2003), p.1494.

[7] X. Wang, X. M. Sun, D. P. Yu, B. S. Zou, Y. D. Li. Adv. Mater.Vol.15(2003),p.1442.

[8] W. J. Li, X. Wang, Y. D. Li. Chem. Comm., Vol.2(2004),p. 164.

[9] X. Wang, Y. D. Li. Angew. Chem. Int. Ed.,Vol.41(2002),p. 4790.

[10] J. J. Song, Qian, Sun, J. B. Liang, X. Li, Y. Cai, Y. Zhang. The Chinese Journal of Process Engineering, Vol.10(2010),p. 950.

[11] Y. X. Li, Y. L. Wu, J. M. Luo, W. L. Sun, G. H. Wang, X. P. Feng. J. Rare Earths., Vol. 24(2006), p. 40.

[12] C.H. Huang., *Science Press*, Beijing, (1997), p. 25.

[13] Y.L. Wu, W. L. Sun, X.Z. Zhou, X. Y. Jiao, J. W. Ding, Y. X. Li. J.Rare Earths,Vol 27(2009), p.767.